



A method for the quantification of the pressure dependent 3D collagen configuration in the arterial adventitia

J.T.C. Schrauwen ^{a,*¹}, A. Vilanova ^{b,1}, R. Rezakhaniha ^{c,2}, N. Stergiopoulos ^{c,2}, F.N. van de Vosse ^{a,1}, P.H.M. Bovendeerd ^{a,1}

^a Cardiovascular Biomechanics, Department of Biomedical Engineering, Eindhoven University of Technology, Eindhoven, The Netherlands

^b BioMedical Image Analysis, Department of Biomedical Engineering, Eindhoven University of Technology, Eindhoven, The Netherlands

^c Laboratory of Hemodynamics and Cardiovascular Technology, Institute of Bioengineering, EPFL, Lausanne, Switzerland

ARTICLE INFO

Article history:

Received 3 May 2012

Received in revised form 30 May 2012

Accepted 12 June 2012

Available online 21 June 2012

Keywords:

Collagen configuration

Adventitia

Pressurized arteries

Carotid artery

MRI-DTI

ABSTRACT

Collagen plays an important role in the response of the arterial wall to mechanical loading and presumably has a load-bearing function preventing overdistension. Collagen configuration is important for understanding this role, in particular in mathematical models of arterial wall mechanics.

In this study a new method is presented to image and quantify this configuration. Collagen in the arterial adventitia is stained with CNA35, and imaged *in situ* at high resolution with confocal microscopy at luminal pressures from 0 to 140 mm Hg. The images are processed with a new automatic approach, utilizing techniques intended for MRI-DTI data. Collagen configuration is quantified through three parameters: the waviness, the transmural angle and the helical angle.

The method is demonstrated for the case of carotid arteries of the white New Zealand rabbit. The waviness indicated a gradual straightening between 40 and 80 mm Hg. The transmural angle was about zero indicating that the fibers stayed within an axial-circumferential plane at all pressures. The helical angle was characterized by a symmetrical distribution around the axial direction, indicating a double symmetrical helix.

The method is the first to combine high resolution imaging with a new automatic image processing approach to quantify the 3D configuration of collagen in the adventitia as a function of pressure.

© 2012 Elsevier Inc. All rights reserved.

1. Introduction

The arterial wall consists of three layers: the intima at the luminal side and subsequently the media and the adventitia. These layers consist of a number of different constituents. Three of those constituents mainly determine the mechanical behavior of the arterial wall: collagen, elastin and smooth muscle cells. Their mechanical characteristics are different: elastin shows compliant linear elastic behavior (Roach and Burton, 1957), collagen has stiff non-linear elastic behavior (Roach and Burton, 1957) and the behavior of smooth muscle cells depends on the extent to which they are activated (Fridze et al., 2001). Also the presence and organization

of those constituents differ per layer. The mechanical response of the wall not only depends on the behavior of individual components but also on their configuration as a whole in each layer. To understand the contribution of each constituent to the mechanical behavior of the entire arterial wall, mathematical models have been designed based on the microstructural configuration (Holzapfel et al., 2000; Machyshyn et al., 2010; Zulliger et al., 2004). To enhance the predictive value of these models, e.g. in predicting the consequences of a pathologic change in one of the constituents (Alford et al., 2008; Baaijens et al., 2010; Kroon and Holzapfel, 2007; Watton and Hill, 2009), quantitative knowledge on the constituents and their mechanical behavior is essential.

In this respect, collagen is of special interest. It is predominantly present in the adventitia as a dense network and is believed to have a load-bearing function, acting as a safety net preventing overdistension of the vessel (Humphrey, 2002). For example, the importance of collagen becomes apparent in aneurysms. Here the collagen configuration evolves continuously and its load-bearing function becomes prominent, up to the point that rupture occurs (Humphrey and Canham, 2000).

* Corresponding author. Present address: Erasmus MC, Biomedical Engineering, Biomechanics Lab, 's-Gravendijkwal 230, Thoraxcenter (Faculty Building), Ee 23.22 Rotterdam, The Netherlands.

E-mail addresses: j.schrauwen@erasmusmc.nl (J.T.C. Schrauwen), A.vilanova@tue.nl (A. Vilanova), Rana.rezakhaniha@gmail.com (R. Rezakhaniha), Nikolaos.stergiopoulos@epfl.ch (N. Stergiopoulos), F.n.v.d.vosse@tue.nl (F.N. van de Vosse), P.h.m.Bovendeerd@tue.nl (P.H.M. Bovendeerd).

¹ Address: Postbus 513, 5600 MB Eindhoven, The Netherlands.

² Address: BM 5125 (Bâtiment AI), Station 17, CH-1015 Lausanne, Switzerland.

Recently work was done on imaging and quantifying the collagen configuration in the adventitia (Chen et al., 2011; Haskett et al., 2010; Rezakhanlha et al., 2011). New findings were reported to demonstrate the importance of microstructural information. However, none of these studies combined high resolution imaging with automatic image processing to quantify both orientation and waviness as a function of pressure. We propose a new combination of techniques in order to quantify the collagen configuration in such a manner.

To demonstrate this method, collagen fibers in the adventitia of two common carotid arteries of the white New Zealand rabbit were imaged. The collagen was imaged *in situ*, while inflating the artery stepwise over a wide pressure range from 0 to 140 mm Hg. The images were processed using a new approach based on transforming microscopy data to mimic MRI-DTI (Diffusion Tensor Imaging) data. This allowed the use of available DTI fiber-tracking techniques (Vilanova et al., 2006) to track the collagen fibers and quantify their configuration in terms of orientation and waviness as a function of pressure.

2. Methods

2.1. Preparation

Common carotid arteries were harvested from two young healthy white New Zealand rabbits of approximately 3.5 kg. The arteries were put in a phosphate-buffered saline (PBS) bath with a 1.5 μ M solution of CNA35–OG488 (Boerboom et al., 2007; Krahn et al., 2006), and kept overnight in an incubator (37°C , 5% CO_2). Labeling with CNA35–OG488 made it possible to visualize the collagen fibers in fresh unfixed tissue (Rezakhanlha et al., 2011). Next the arteries were washed in a PBS bath and immediately imaged under a microscope or stored overnight PBS solution at 4°C . The maximum time between harvesting and the start of the measurement was less than 48 h.

From the arteries sections with a length of 1.5–2 cm were taken. The sections were mounted on a frame between two metal tubes and fixed with suture wire. An axial stretch of 1.4 was applied (Fonck et al., 2007; van den Broek et al., 2011) and the bath, the PBS and the space surrounding the bath and the microscope stage were kept at 37°C to mimic *in vivo* conditions (Fig. 1).

Subsequently sodium nitroprusside was added to a concentration of 10^{-6} M in the bath. This addition ensured that all smooth muscle cells became completely relaxed and the wall had consistent passive mechanical behavior. The tubes from the frame were

then connected to a reservoir that was connected to a syringe pump. In this closed system the syringe pump was used to inflate the artery and enable the measurement of the collagen configuration *in situ* at a precise pressure. The last step in the preparation process was pre-conditioning the arteries with five cycles of 0–120–0 mm Hg at a rate of approximately 1.5 mm Hg/s.

2.2. Imaging

The imaging of the arterial wall was conducted with confocal laser microscopy using an upright Leica SP2 and a $63\times$ water immersed lens with a field of view of 238 by 238 μm . The collagen was excited by a laser with a 488 nm wavelength. Its emission was measured within the 500–550 nm range. The collagen was measured throughout the adventitia at planes with increasing depth from the outer surface with steps of 0.5 μm . The maximum depth was determined as the deepest point that still had signal. The individual images of the planes were combined into a 3D image with the commercial software package Imaris (Bitplane, Switzerland).

The collagen configuration of the arteries was visualized between 0 and 80 mm Hg at pressure steps of 5 mm Hg, and between 80 and 140 mm Hg at pressure steps of 10 mm Hg. The mean physiological arterial pressure of these rabbits is approximately 70 mm Hg. Due to the inflation of the artery the area of interest could shift out of the field of view. Therefore after each pressure step the position of the stage was manually adjusted to ensure that approximately the same area of the adventitia was visualized.

2.3. Image analysis

To quantify the configuration of the collagen fibers in the 3D microscopy images, we employed techniques that have been developed to visualize and track fiber-like structures in MRI-DTI data. MRI-DTI measurements are based on the diffusion of water that is described by a diffusion tensor \mathbf{D} (Eq. (1)), which is a symmetric positive definite matrix:

$$\mathbf{D} = D_{ij}\mathbf{e}_i\mathbf{e}_j \quad \text{for } i,j = x,y,z \quad (1)$$

where \mathbf{e}_x , \mathbf{e}_y and \mathbf{e}_z are unit vectors that form a Cartesian basis, D_{ij} are the components with respect to this basis (Einstein notation), and $\mathbf{e}_i\mathbf{e}_j$ represents the tensor product of two unit vectors. The diffusion tensor \mathbf{D} can also be written in terms of eigenvalues (λ_1 , λ_2 , and λ_3) and unit vectors corresponding to the eigenvectors (\mathbf{e}_1 , \mathbf{e}_2 and \mathbf{e}_3):

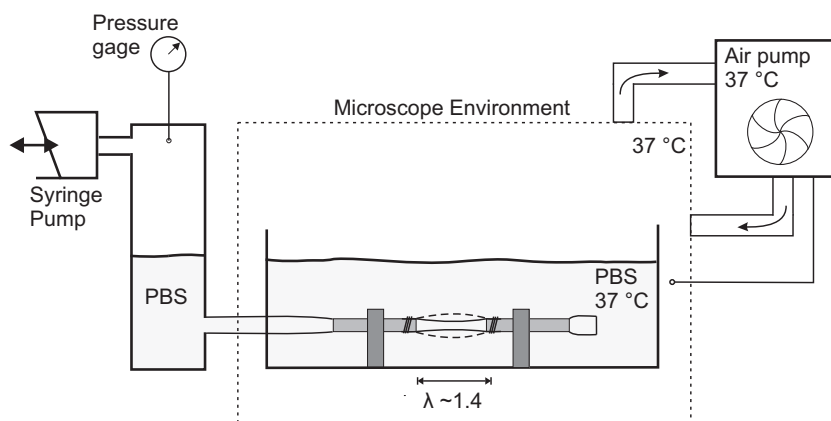


Fig. 1. Experimental setup under a confocal microscope used to image the collagen configuration at different pressures. The pressure was regulated by a syringe pump, which allowed the pressure in the artery to be set at the desired level during imaging. The environment was kept at 37°C and an axial stretch of 1.4 was applied.

$$\mathbf{D} = \lambda_1 \mathbf{e}_1 \mathbf{e}_1 + \lambda_2 \mathbf{e}_2 \mathbf{e}_2 + \lambda_3 \mathbf{e}_3 \mathbf{e}_3 \quad (2)$$

The eigenvector with the largest eigenvalue is considered to represent the local diffusion direction. This direction is used by a fiber tracking method to reconstruct the fibrous structure. A more elaborate description can be found in Vilanova et al. (2006).

In order to apply fiber tracking techniques developed for DTI to microscopy images, a tensor with similar information as the diffusion tensor had to be derived from the images, i.e. the tensor should describe the local orientation of the fibrous structure at each point. We used the Hessian \mathbf{H} defined as a matrix with second order derivatives of the image intensity $I(x, y, z)$ (Florack et al., 1992):

$$\mathbf{H} = H_{ij} \mathbf{e}_i \mathbf{e}_j \quad \text{for } i, j = x, y, z \quad (3)$$

with its components H_{ij} defined as:

$$H_{xx} = \frac{\partial^2 I}{\partial x \partial x}, \quad H_{xy} = \frac{\partial^2 I}{\partial x \partial y}, \dots, H_{zz} = \frac{\partial^2 I}{\partial z \partial z} \quad (4)$$

In this study the second order derivatives for the Hessian were estimated by convolving (*) an image twice with first order Gaussian derivatives:

$$\hat{H}_{ij} = G_i * G_j * I \quad \text{for } i, j = x, y, z \quad (5)$$

This results in an estimate of the Hessian ($\hat{\mathbf{H}}$) for each voxel in the data set. The first order Gaussian derivatives were defined as:

$$G_i = \frac{-i}{\sigma^2 \sqrt{2\pi\sigma^2}} e^{-\frac{x^2+y^2+z^2}{2\sigma^2}} \quad \text{for } i = x, y, z \quad (6)$$

Here σ controls the width of the kernel. The width of the kernel correlates to how effectively a structure with a specific width can be detected (Frangi et al., 1998). In this study $\sigma = 2$ pixels was chosen. A pilot study showed that this corresponded well to the approximate mean width of fibers in the images. The Hessian can also be written in terms of its eigenvalues (λ_1^H, λ_2^H and λ_3^H) and unit vectors along its eigenvectors ($\mathbf{e}_1, \mathbf{e}_2$ and \mathbf{e}_3):

$$\hat{\mathbf{H}} = \lambda_1^H \mathbf{e}_1 \mathbf{e}_1 + \lambda_2^H \mathbf{e}_2 \mathbf{e}_2 + \lambda_3^H \mathbf{e}_3 \mathbf{e}_3 \quad (7)$$

Equivalent to DTI data processing, the main direction in each voxel of image I can be found by an eigenanalysis of $\hat{\mathbf{H}}$. However, since the eigenvectors derived from the Hessian are based upon the intensity difference, the eigenvector belonging to the largest eigenvalue λ_1^H will be perpendicular to the fiber. To allow processing with the existing DTI fiber tracking techniques the main eigenvector should be parallel to the fiber. For this reason the absolute eigenvalues were inverted while keeping the eigenvectors the same. The inversion lead to a so called pseudo diffusion tensor \mathbf{D}' suited for DTI processing techniques.

$$\mathbf{D}' = \frac{1}{|\lambda_1^H + 1|} \mathbf{e}_1 \mathbf{e}_1 + \frac{1}{|\lambda_2^H + 1|} \mathbf{e}_2 \mathbf{e}_2 + \frac{1}{|\lambda_3^H + 1|} \mathbf{e}_3 \mathbf{e}_3 \quad (8)$$

The inversion causes the main eigenvector of \mathbf{D}' to be parallel to the fiber direction. Finally, the tensor \mathbf{D}' was used as input for the DTI software vIST/e developed by the Bio-Medical Image Analysis group at TU/e (<http://bmia.bmt.tue.nl/software/VISTE/>). The image processing resulted in multiple 3D fiber tracings per collagen fiber (Fig. 4, Bottom).

2.4. Quantification of the collagen configuration

The configuration of a tracing within a fiber was quantified by three parameters (Fig. 2):

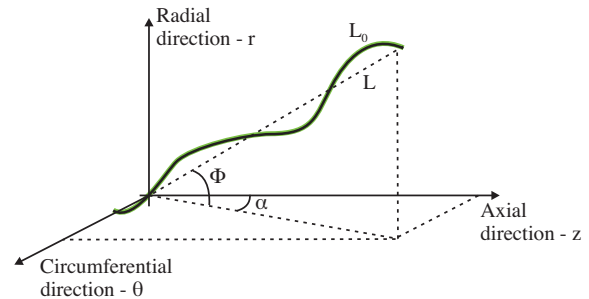


Fig. 2. Three parameters were used to define the configuration of a single fiber: waviness $w = L/L_0$, transmural angle φ and helical angle α .

- Waviness w defined as the ratio between the Euclidean length L , measured straight from the beginning to the end, and the whole length L_0 along the fiber: $w = L/L_0$.
- The transmural angle φ defined as the angle of a fiber to cross over between the inside and the outside of the arterial wall in radial direction measured with respect to the axial-circumferential plane.
- The helical angle α defined as the angle between the axial direction and the projection of the fiber vector onto the axial-circumferential plane.

For each parameter a histogram was created from all the fiber tracings within a 3D data set. The histograms of the waviness were characterized by the fraction of fibers that was (almost) completely straightened $w \geq 0.9$. Probability density functions (PDF) were fitted on the histograms of the transmural and helical angles in order to characterize them. The histograms of the transmural angle φ were characterized by two parameters φ_1 and σ from the circular distribution:

$$f_\varphi(\varphi; \varphi_1, \sigma) = A e^{\frac{\cos[2(\varphi-\varphi_1)]+1}{\sigma}} \quad (9)$$

with main transmural angle φ_1 and width σ . The distribution was normalized by the factor A .

For the helical angle a bimodal circular distribution (Driessens et al., 2005) was chosen because a double helix was expected:

$$f_\alpha(\alpha; \alpha_1, \alpha_2, \sigma_1, \sigma_2) = A \left(e^{\frac{\cos[2(\alpha-\alpha_1)]+1}{\sigma_1}} + e^{\frac{\cos[2(\alpha-\alpha_2)]+1}{\sigma_2}} \right) \quad (10)$$

The distribution for α was characterized by four parameters: α_1, α_2 for the main angles and σ_1, σ_2 for the widths of the distribution. The values were determined by the best fit of the PDF onto the histogram. The distributions, and therefore the parameters of the fits, change as a function of pressure. Hence, the change of the PDF parameters is a direct quantitative description of how the collagen network changes due to pressure.

3. Results

Fig. 3 shows that the fluorescent CNA35 probe in combination with confocal microscopy allowed for a detailed visualization of the collagen network in the adventitia. In the images individual collagen bundles can clearly be distinguished. The depth from the outer surface at which collagen could be imaged decreased with the pressure from approximately 80 μm at 0 mm Hg to 50 μm at 140 mm Hg.

Fig. 3 shows images from sample 1 obtained at pressures between 0 and 140 mm Hg. Up to 60 mm Hg the collagen fibers are wavy. At 60 and 80 mm Hg the fibers get straightened gradually and shift towards a more circumferential orientation. Above 80 mm Hg almost all fibers are completely straightened. In the

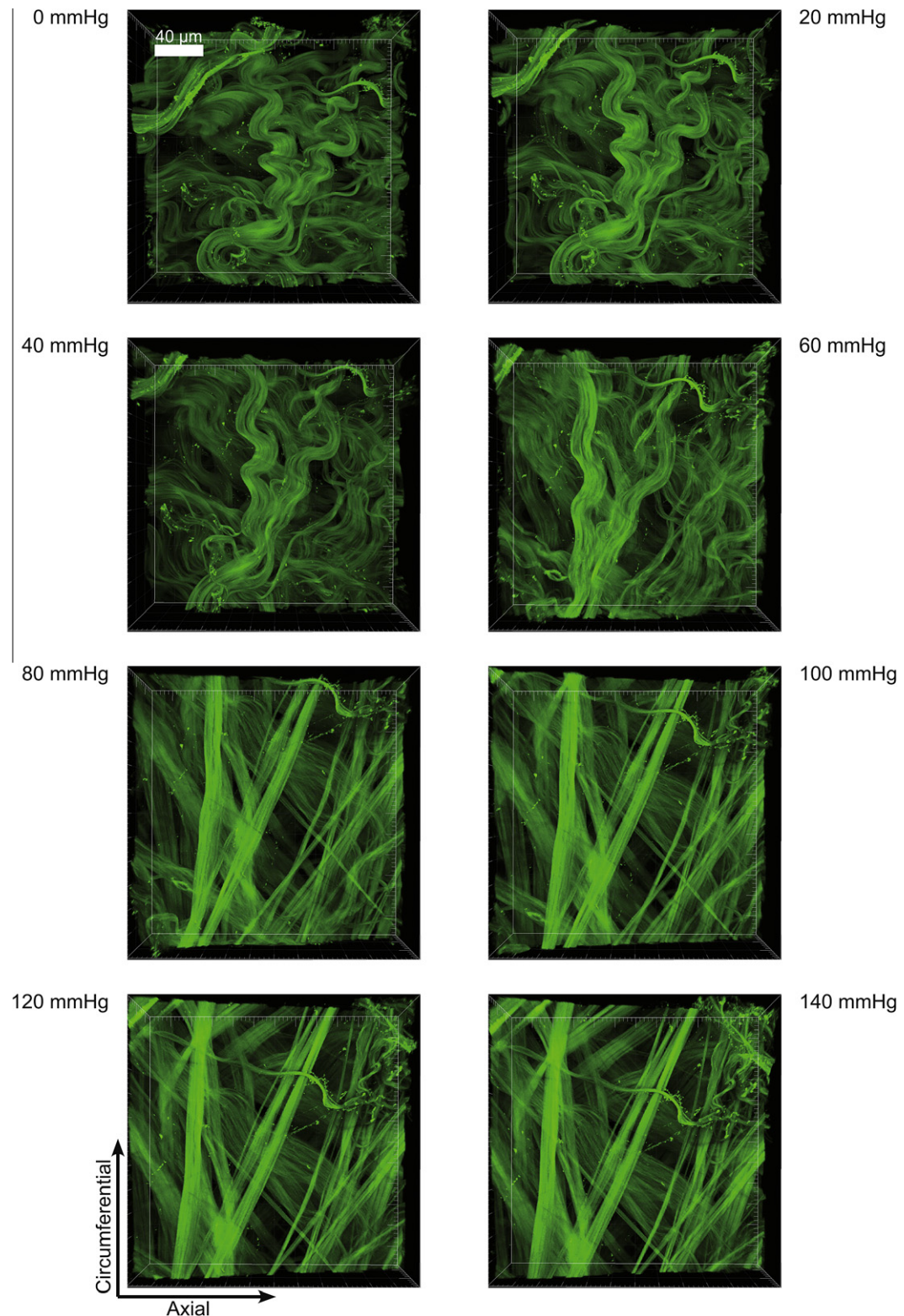


Fig. 3. Collagen fibers in the adventitia of the carotid artery (sample 1). The same area was imaged at different pressure steps from 0 to 140 mm Hg; eight intermediate steps are shown. The gradual straightening of (individual) fibers is observed. The biggest configuration change mainly occurs between 40 and 80 mm Hg.

online resources a movie with all consecutive pressure steps is included that makes the effect of the increasing pressure more insightful. **Fig. 3** and the movie both clearly show the configuration change.

With the image processing approach it was possible to quantify the properties of the collagen network. **Fig. 4** shows an example of

a section of a microscopy image and the result from the fiber tracking. Both are three dimensional reconstructions. The fiber tracking shows a good resemblance with the original image: the main structures and the overall configuration are found. Yet there are some reoccurring deviations from the original image. Fibers close to the border or with a low intensity are not always found (**Fig. 4**,

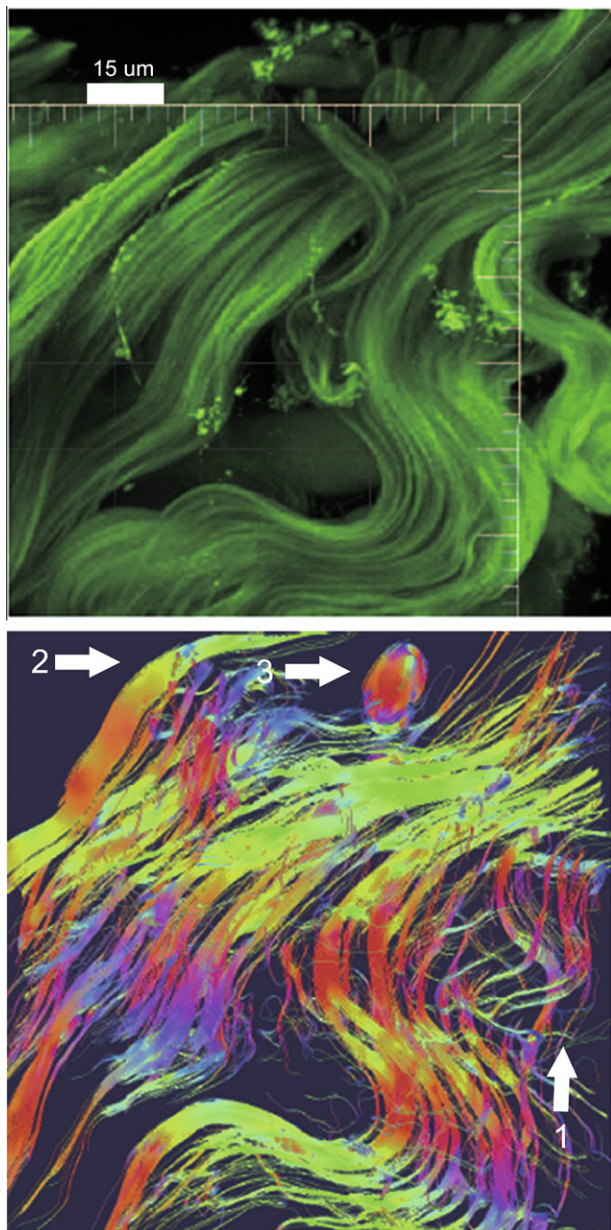


Fig. 4. Comparison of a 3D microscopy image section at 0 mm Hg (top) with the result of the fiber tracking using the image processing technique (bottom). The green color indicates an axial (horizontal) direction. Red indicates the circumferential (vertical) direction. Blue indicates a radial direction, perpendicular to the page. The main structures and overall configuration of the collagen were found. The arrows point out details explained in the text.

arrow 1) and fibers with a high intensity may show up disproportionately thick (arrow 2). Some fibers are detected but their shape is not correctly represented, e.g. a pitch is found but represented as globular shape (arrow 3).

Fig. 5 shows examples of the distribution density of the configuration at 0, 40, 80 and 120 mm Hg and the corresponding microscopy images. In the left column the waviness distributions are plotted. A shift towards one is observed due to the pressure increase, indicating fiber straightening. The middle column shows that the transmural angle is centered around 0° at all pressures. In the right column at 80 and 120 mm Hg a double symmetrical distribution at approximately ±70° appears for the helical angle.

The distributions for all pressure steps were summarized in Fig. 6. The top left of Fig. 6 shows the waviness change due to

pressure. In both samples the fibers get straightened between 40 and 80 mm Hg. The top right of Fig. 6 shows the transmural angle as a function of pressure. The transmural angle (solid lines) is centered around 0° for all pressures. This implies that the fibers remain within an axial-circumferential plane around the axis. However, below 60 mm Hg a relatively wide distribution is found for both samples (Dashed lines). The bottom figures show the changing helical angle distribution as a function of pressure for both samples. The solid lines depict the main orientations and the width is indicated by the filled area. The double symmetrical helix appears in both samples above 60 mm Hg at approximately ±70°. Below 60 mm Hg two main orientations could not be found because the distributions were too wide.

4. Discussion

In this study we imaged the collagen network of the adventitia of the common carotid artery of the rabbit in high detail and observed its change in configuration as a function of pressure. Collagen was imaged *in situ* at small subsequent pressure steps, which made it possible to compare the same area at different pressures. Thus, the effect of increasing pressure on individual fibers and on the network as a whole could be analyzed.

A new image processing approach was developed because no method was readily available to automatically quantify the waviness of fibers. By applying a DTI fiber tracking technique the whole fiber path within the data set could be reconstructed. This allowed us to determine the waviness of the fibers. An additional benefit is that the orientation is determined over the whole fiber in the data set, instead of using each individual point on the fiber as done in previous studies. This provides a robust measurement which is less sensitive to local variations.

The gradual straightening of individual fibers *in situ*, as quantified through the waviness distribution was not observed *in situ* and quantified up to now. We observed that the collagen network got straightened around physiological pressure (rabbits). At 60 mm Hg the collagen fibers started to get completely straightened and above 100 mm Hg the whole network was predominately straightened. Fonck et al. investigated the pressure–radius curve of the same type of artery as used in this study. They observed that the vessel distention starts to level off from approximately 60 mm Hg and reaches its maximum around 100 mm Hg. This is in agreement with our study and supports the idea that the collagen fibers prevent overdistension of the wall above physiological pressure. Thus our study gives insight in how the behavior of the vessel at the macroscopic level is coupled to its microstructure. We found a symmetrical double helix with a mean angle for the whole adventitia of approximately ±70° at 70 mm Hg (mean arterial pressure) and above with an axial stretch of 1.4. The transmural angle was about zero indicating that the fibers stayed within an axial-circumferential plane at all pressures. The collagen configuration was thus quantified by the orientation and waviness of the collagen fibers as a function of pressure.

Other studies already developed methods to quantify the collagen orientation in the adventitia (Canham et al., 1997; Finlay et al., 1995; Rezakhanlou and Stergiopoulos, 2008; Wicker et al., 2008). In a recent study by Chen et al. (2011) a method is presented that also gives the orientation and waviness of the collagen fibers at different pressures. However, here the waviness was determined manually and only a normalized helical angle was reported. Also the measured arteries were not intact because the media and intima were removed. Another recent study done by Keyes et al. (2011) reported a helical angle as a function of the pressure, but did not determine the waviness of the collagen fibers. Our method presented here improved upon these points.

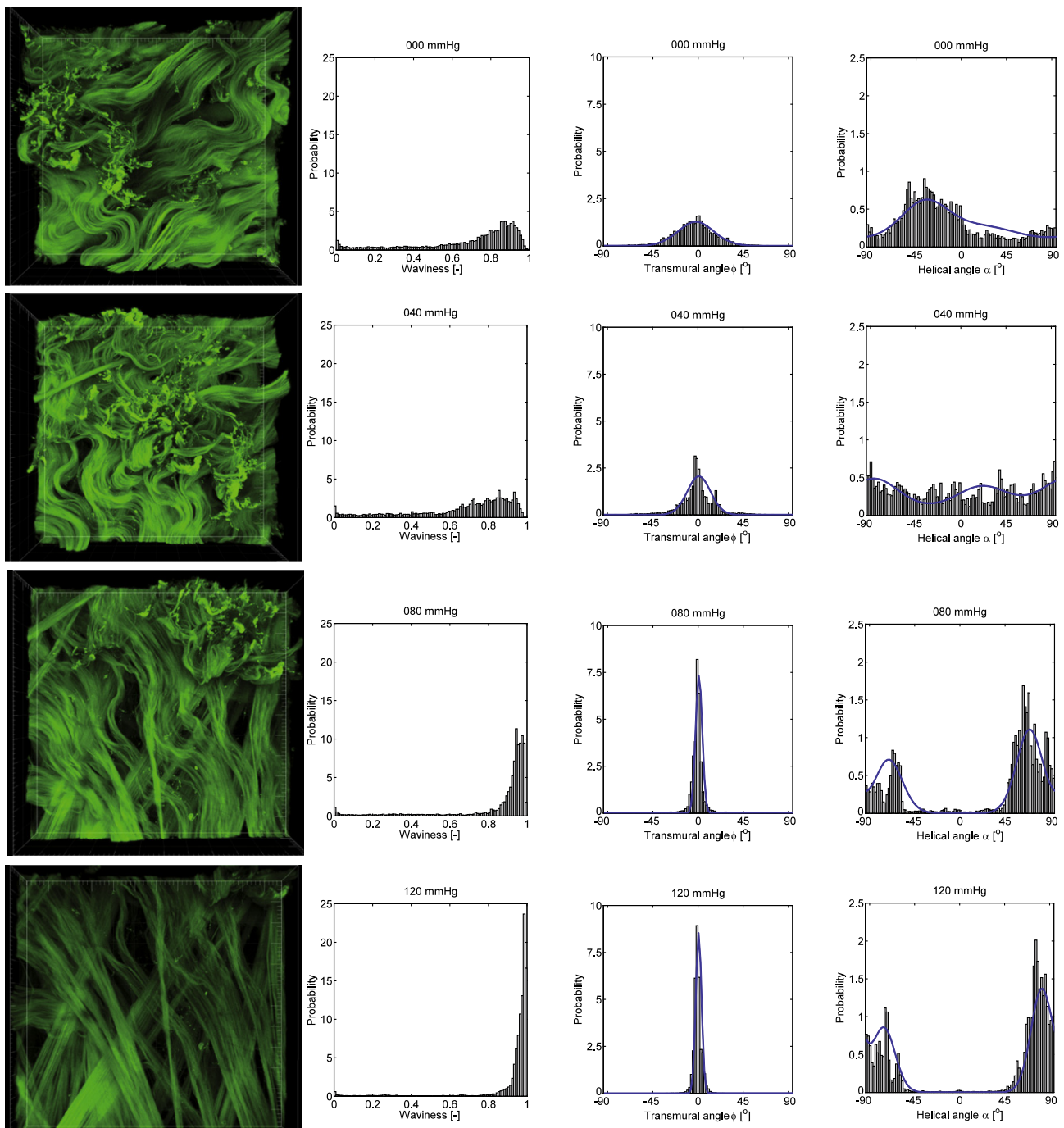


Fig. 5. The probability density distributions of the waviness, the transmural angle and the helical angle distributions at 0, 40, 80 and 120 mm Hg of sample 2. Due to the increase in pressure the waviness distribution shifts towards 1, indicating that the fibers get straightened. The transmural angle remains around zero, and thus the fibers stay within a constant plane around the axis. In the helical angle distribution a double symmetrical angle appears at 80 and 120 mm Hg. The PDFs (Eqs. (9) and (10)) that were fitted on the transmural and helical angle distributions are also plotted.

To demonstrate our method we used two common carotid arteries of rabbits, which is an elastic artery type. The helical angle of the collagen fibers found in our study was approximately $\pm 70^\circ$ at physiological pressure. This is consistent with the near circumferential orientation of collagen fibers observed in other elastic arteries, e.g. in the mouse aorta (Keyes et al., 2011), the human aorta (Haskett et al., 2010) and the proximal porcine carotid and the rabbit carotid (Sokolis et al., 2011).

The quantification of the collagen configuration in the arterial wall is essential for the modeling of mechanics, growth and

remodeling of the arterial wall. Models based on such microstructural information are expected to provide more insight in the mechanical function of the arterial wall (Holzapfel et al., 2000). Microstructural models also enable a description of the remodeling of the arterial wall, in response to disease or changed hemodynamic conditions, in terms of changes in collagen orientation and waviness (Alford et al., 2008; Baaijens et al., 2010; Kroon and Holzapfel, 2007; Machyshyn et al., 2010; Watton and Hill, 2009). The parameters of the collagen configuration of any specific artery can be found by applying the combination of techniques shown here to

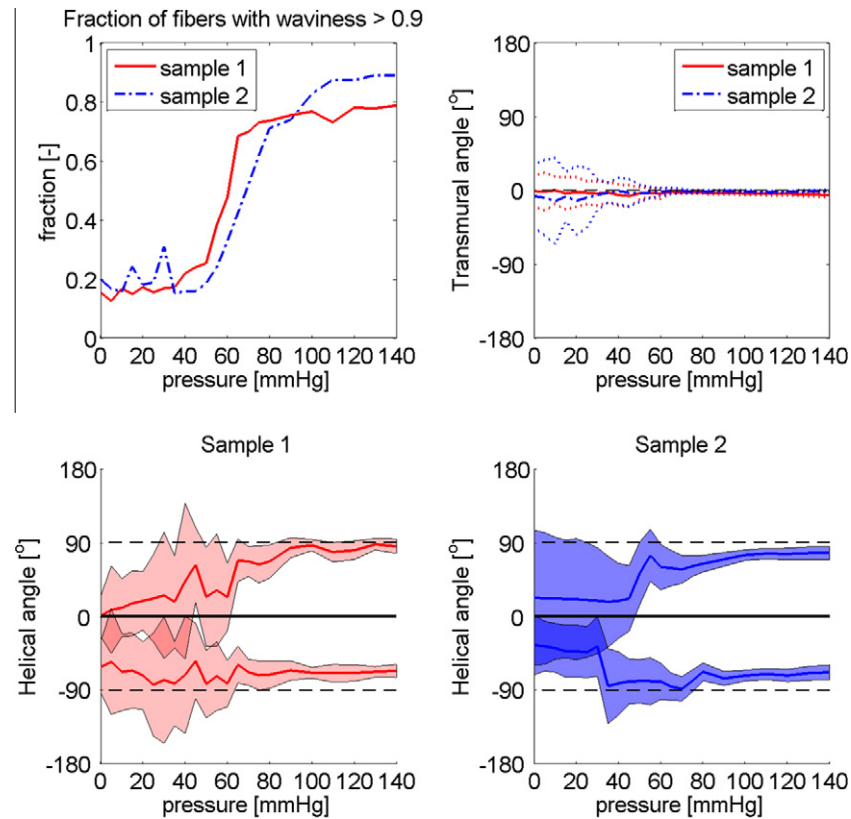


Fig. 6. (Top left) Fraction of fibers that are (almost) straightened ($w \geq 0.9$) as a function of pressure. In both samples most of the fibers got straightened between 40 and 80 mm Hg. Below 40 mm Hg both samples have a wavy configuration, while above 80 mm Hg the fibers were predominately straightened. (Top right) The circular distribution of the transmural angle as a function of pressure from fits by Eq. (9). The transmural angle (solid lines) remains around 0° throughout the whole pressure range. The width (dashed lines) of the distribution becomes almost none existing above physiological pressure. (Bottom) Circular distribution of the helical angle. The solid lines represent the main helical angles α_1 and α_2 per sample from the fits of Eq. (10). The filled area represents the width of the distribution σ_1 and σ_2 for the corresponding angle. In both samples, above physiological pressure two symmetrical angles appear with a small distribution and are oriented towards nearly the circumferential direction. For representation purposes the circular distributions are plotted from $-180^\circ \leq \alpha \leq 180^\circ$. Note that -90° and 90° both denote circular orientation.

a number of samples. Our findings support the assumption, used in many models, that the collagen fibers are organized in a double-symmetrical helix (Badel et al., 2012; Driessens et al., 2005; Holzapfel et al., 2000; Sokolis et al., 2011; Sommer and Holzapfel, 2012; van den Broek et al., 2011). Our results also support the assumption that fibers are located within the axial–circumferential plane. The observed and quantified gradual straightening can be used to create a model of arterial wall mechanics that accounts for collagen waviness (Lanir, 1983; Rezakhaniha and Stergiopoulos, 2008; Zulliger et al., 2004). Obviously, more vessels must be examined to substantiate our findings. The possibility to measure more complex geometries, for example bifurcations, should also be explored. These are common sites for atherosclerotic plaques to develop, therefore making them especially interesting for modeling and remodeling studies (Creane et al., 2012). Another possible area of application includes the study of collagen remodeling in hydrogels (Nagel and Kelly, 2012).

It should be noted that choices were made in order to observe and quantify the collagen configuration. The width of the field of view was chosen at 238 μm which is small as compared to the diameter of the artery but large as compared to the average diameter of the collagen fibers. Thus the changes of the collagen network were observed at a microstructural level. We aimed to image exactly the same area at subsequent pressure steps. However, we may not have been able to completely correct for the shifting and stretching of the tissue with increasing pressure. This could compromise the analysis between consecutive pressure steps and might explain the alternating value of the straightened fiber fraction of sample 2 between 0 and 40 mm Hg (Fig. 6 top left).

For the image analysis choices were made as well. We use a fixed kernel size of $\sigma = 2$ pixels (Eq. (6)) but a method with a variable kernel size would be able to detect fibers of different diameters more efficiently (Frangi et al., 1998). Secondly, to obtain the pseudo diffusion tensor (\mathbf{D}') 1 was added in the denominator (Eq. (8)). This can distort the ratio of the eigenvalues and therefore also the fiber tracking method (Vilanova et al., 2006). As opposed to the diffusion tensor the Hessian can have negative eigenvalues. Therefore the absolute value of the eigenvalues was taken and thus no distinction could be made between points in areas going from light to dark or from dark to light (Frangi et al., 1998). This created the possibility that the background could be seen as a fibrous structure and was traced as such.

5. Conclusion

In conclusion, in this study we presented a new combination of high resolution imaging and automatic image processing to quantify the collagen configuration in the arterial adventitia as a function of pressure. The approach and results shown in this study provide a good starting point for modeling of arterial wall mechanics based on the microstructure.

Acknowledgment

We would like to thank Prof. C.V.C. Bouten for providing the CNA35–OG488 probe.

Appendix A. Supplementary data

Supplementary data associated with this article can be found, in the online version, at <http://dx.doi.org/10.1016/j.jsb.2012.06.007>.

References

- Alford, P.W., Humphrey, J.D., Taber, L.A., 2008. Growth and remodeling in a thick-walled artery model: effects of spatial variations in wall constituents. *Biomech. Model. Mechanobiol.* 7 (4), 245–262.
- Baaijens, F.P.T., Bouten, C.V.C., Driessens, N.J.B., 2010. Modeling collagen remodeling. *J. Biomech.* 43 (1), 166–175.
- Badel, P., Avril, S., Lessner, S., Sutton, M., 2012. Mechanical identification of layer-specific properties of mouse carotid arteries using 3D-DIC and a hyperelastic anisotropic constitutive model. *Comput. Methods Biomed. Eng.* 15 (1), 37–48.
- Borboon, R.A., Krahn, K.N., Megens, R.T.A., van Zandvoort, M.A.M.J., Merkx, M., Bouting, C.V.C., 2007. High resolution imaging of collagen organization and synthesis using a versatile collagen specific probe. *J. Struct. Biol.* 159 (3), 392–399.
- Canham, P.B., Finlay, H.M., Boughner, D.R., 1997. Contrasting structure of the saphenous vein and internal mammary artery used as coronary bypass vessels. *Cardiovasc. Res.* 34 (3), 557–567.
- Chen, H., Liu, Y., Slipchenko, M.N., Zhao, X., Cheng, J.X., Kassab, G.S., 2011. The layered structure of coronary adventitia under mechanical load. *Biophys. J.* 101 (11), 2555–2562.
- Creane, A., Maher, E., Sultan, S., Hynes, N., Kelly, D.J., Lally, C., 2012. A remodelling metric for angular fibre distributions and its application to diseased carotid bifurcations. *Biomech. Model. Mechanobiol.* 11 (6), 869–882.
- Driessens, N.J.B., Bouting, C.V.C., Baaijens, F.P.T., 2005. A structural constitutive model for collagenous cardiovascular tissues incorporating the angular fiber distribution. *J. Biomech. Eng.* 127 (3), 494–503.
- Finlay, H., McCullough, L., Canham, P., 1995. Three-dimensional collagen organization of human brain arteries at different transmural pressures. *J. Vasc. Res.* 32 (5), 301–312.
- Florack, L.M.J., ter Haar Romeny, B.M., Koenderink, J.J., Viergever, M.A., 1992. Scale and the differential structure of images. *Image Vis. Comput.* 10 (6), 376–388.
- Fonck, E., Prod'hom, G., Roy, S., Augsburger, L., Rüfenacht, D.A., Stergiopoulos, N., 2007. Effect of elastin degradation on carotid wall mechanics as assessed by a constituent-based biomechanical model. *Am. J. Physiol. Heart Circ. Physiol.* 292 (6), H2754–H2763.
- Frangi, A., Niessen, W., Vincken, K., Viergever, M., 1998. Multiscale vessel enhancement filtering. *Med. Image Comput. Comput. Assist. Interv.* 1496, 130–137.
- Fridz, P., Makino, A., Miyazaki, H., Meister, J.J., Hayashi, K., Stergiopoulos, N., 2001. Short-term biomechanical adaptation of the rat carotid to acute hypertension: contribution of smooth muscle. *Ann. Biomed. Eng.* 29 (1), 26–34.
- Haskett, D., Johnson, G., Zhou, A., Utzinger, U., Vande Geest, J., 2010. Microstructural and biomechanical alterations of the human aorta as a function of age and location. *Biomechanics and Modeling in Mechanobiology.* 9 (6), 725–736.
- Holzapfel, G.A., Gasser, T.C., Ogden, R.W., 2000. A new constitutive framework for arterial wall mechanics and a comparative study of material models. *J. Elast.* 61 (1), 1–48.
- Humphrey, J., Canham, P., 2000. Structure, mechanical properties, and mechanics of intracranial saccular aneurysms. *J. Elast.* 61 (1), 49–81.
- Humphrey, J.D., 2002. *Cardiovascular Solid Mechanics: Cells Tissues and Organs*. Springer, Verlag.
- Keyes, J.T., Haskett, D.G., Utzinger, U., Azhar, M., Geest, J.P.V., 2011. Adaptation of a planar microbiaxial optomechanical device for the tubular biaxial microstructural and macroscopic characterization of small vascular tissues. *J. Biomech. Eng.* 133 (7), 075001.
- Krahn, K.N., Bouting, C.V.C., Van Tuijl, S., Van Zandvoort, M.A.M.J., Merkx, M., 2006. Fluorescently labeled collagen binding proteins allow specific visualization of collagen in tissues and live cell culture. *Anal. Biochem.* 350 (2), 177–185.
- Kroon, M., Holzapfel, G.A., 2007. A model for saccular cerebral aneurysm growth by collagen fibre remodelling. *J. Theor. Biol.* 247 (4), 775–787.
- Lanir, Y., 1983. Constitutive equations for fibrous connective tissues. *J. Biomech.* 16 (1), 1–12.
- Machyshyn, I., Bovendeerd, P.H.M., van de Ven, A.A.F., Rongen, P.M.J., van de Vosse, F., 2010. A model for arterial adaptation combining microstructural collagen remodeling and 3D tissue growth. *Biomech. Model. Mechanobiol.* 9 (6), 671–687.
- Nagel, T., Kelly, D.J., 2012. Remodelling of collagen fibre transition stretch and angular distribution in soft biological tissues and cell-seeded hydrogels. *Biomech. Model. Mechanobiol.* 11 (3–4), 325–339.
- Rezakhanlou, R., Agianniotis, A., Schrauwen, J.T.C., Griffa, A., Sage, D., Bouting, C.V.C., van de Vosse, F., Unser, M., Stergiopoulos, N., 2011. Experimental investigation of collagen waviness and orientation in the arterial adventitia using confocal laser scanning microscopy. *Biomech. Model. Mechanobiol.* 11, 461–473.
- Rezakhanlou, R., Stergiopoulos, N., 2008. A structural model of the venous wall considering elastin anisotropy. *J. Biomech. Eng.* 130, 031017.
- Roach, M.R., Burton, A.C., 1957. The reason for the shape of the distensibility curves of arteries. *Can. J. Biochem. Physiol.* 35 (8), 681–690.
- Sokolis, D.P., Sassani, S., Kritharis, E.P., Tsangaris, S., 2011. Differential histomechanical response of carotid artery in relation to species and region: mathematical description accounting for elastin and collagen anisotropy. *Med. Biol. Eng. Compu.* 49 (8), 867–879.
- Sommer, G., Holzapfel, G.A., 2012. 3D constitutive modeling of the biaxial mechanical response of intact and layer-dissected human carotid arteries. *J. Mech. Behav. Biomed. Mater.* 5 (1), 116–128.
- van den Broek, C.N., van der Horst, A., Rutten, M.C.M., van de Vosse, F.N., 2011. A generic constitutive model for the passive porcine coronary artery. *Biomech. Model. Mechanobiol.* 10 (2), 249–258.
- Vilanova, A., Zhang, S., Kindermann, G., Laidlaw, D., 2006. An introduction to visualization of diffusion tensor imaging and its applications. In: *Visualization and Processing of Tensor Fields*. Springer Verlag series, Mathematics and Visualization, pp. 121–153.
- Watton, P., Hill, N., 2009. Evolving mechanical properties of a model of abdominal aortic aneurysm. *Biomech. Model. Mechanobiol.* 8 (1), 25–42.
- Wicker, B., Hutchens, H., Wu, Q., Yeh, A., Humphrey, J., 2008. Normal basilar artery structure and biaxial mechanical behavior. *Comput. Methods Biomed. Eng.* 11 (5), 539–551.
- Zulliger, M.A., Fridz, P., Hayashi, K., Stergiopoulos, N., 2004. A strain energy function for arteries accounting for wall composition and structure. *J. Biomech.* 37 (7), 989–1000.